



Final Draft **of the original manuscript**

Klein, O.; Zimmermann, T.; Pröfrock, D.:

Improved determination of technologically critical elements in sediment digests by ICP-MS/MS using N₂O as a reaction gas.

In: Journal of Analytical Atomic Spectrometry. Vol. 36 (2021) 7, 1524 - 1532.

First published online by RSC: 19.05.2021

<https://dx.doi.org/10.1039/D1JA00088H>

Improved Determination of Technologically Critical Elements in Sediment digests by ICP- MS/MS using N₂O as Reaction gas

*Ole Klein^{a,b}, Tristan Zimmermann^a and Daniel Pröfrock^a **

^a Helmholtz-Zentrum Geesthacht, Institute of Coastal Environmental Chemistry, Max-Planck
Str. 1, 21502 Geesthacht, Germany

^b Universität Hamburg, Department of Chemistry, Inorganic and Applied Chemistry, Martin-
Luther-King-Platz 6, 20146 Hamburg, Germany

Tel.: +49 4152 87 2846

Fax: +49 4152 87 1875

*Corresponding author: daniel.proefrock@hzg.de

1
2
3
4
5
6
7
8
9
10
11
12
13
14
15
16
17
18
19
20
21
22
23
24
25
26
27
28
29
30
31
32
33
34
35
36
37
38
39
40
41
42
43
44
45
46
47
48
49
50
51
52
53
54
55
56
57
58
59
60

21 **Keywords**

22 Environmental analysis, sediment reference materials, spectral interference reduction, ultra-
23 trace analysis

24 **Abstract**

25 The investigation of technologically critical elements (TCEs) as emerging pollutants is a
26 constantly growing field of environmental research and societal concern. Nevertheless, existing
27 data for most TCEs are still unsatisfactory for an accurate assessment of their potential
28 (eco)toxicological effects on humans and the environment. The limited availability of data
29 mainly results from the technical challenging analysis of selected TCEs. Low concentrations
30 of TCEs in environmental matrices ($\mu\text{g kg}^{-1}$ or lower) and the associated complex and time-
31 consuming sample preparation pose the greatest challenges. This work aims at developing a
32 new ICP-MS/MS-based multi-elemental approach targeting the analysis of all major TCEs (Sc,
33 Ga, Ge, Nb, In, Te, La, Ce, Pr, Nd, Sm, Eu, Gd, Tb, Dy, Yb, Lu, Ta) in sediment, which
34 represents one of the most important matrices for environmental research. N_2O is applied as
35 reaction gas to overcome possible spectral interferences during ICP-MS/MS analysis. The use
36 of N_2O as reaction gas for ICP-MS/MS analysis enabled higher oxide-product ion yields for
37 many TCEs in comparison to the frequently used O_2 cell gas. Hence, selectivity and sensitivity
38 of the method were improved. The presented multi-element method using N_2O as reaction gas
39 achieved *LODs* between $0.00023 \mu\text{g L}^{-1}$ (Eu) and $0.13 \mu\text{g L}^{-1}$ (Te) for all analyzed TCEs.
40 Likewise, for all analyzed elements, except for Te, recoveries between 80% and 112% were
41 obtained for at least one of the analyzed reference materials (GBW 07313, GBW 07311, and
42 BCR-2).

43

44 Introduction

45 Technologically critical elements (TCEs) are defined as elements or minerals, which can be
46 considered socially and economically critical, due to possible supply risks or supply
47 restrictions. Despite the potentially limited and critical supply situation, TCEs play a crucial
48 role for today's high tech applications.¹⁻⁴ TCEs are used in various industrial sectors including,
49 the information technology sector, the transport sector (electromobility), and the field of
50 renewable energy production (wind power, solar power etc.)^{5, 6}. However, they are also present
51 in almost every multimedia device and consequently becoming mandatory in every single
52 household. Despite the increasing interest in and usage of TCEs in modern industries, some of
53 these elements (e.g. Ga, Ge, Nb, In, Te and Ta) still show a lack of knowledge regarding their
54 potential impact on the environment.^{1, 7} Up to now, little is known about the (eco)toxicity of
55 many TCEs and their respective environmental species. It is believed, that the rising usage of
56 TCEs may lead to unforeseen negative environmental impacts within the next years or
57 decades.⁷⁻⁹ Due to the challenging analytical determination of selected TCEs recent
58 environmental studies still show a deficiency of related data.¹⁰ Consequently, there is an
59 increasing demand for adequate and reliable analytical methods for the determination of TCEs
60 in typical environmental matrices such as water, biota or sediments.^{2, 7}

61 In the first place, the analysis of TCEs in environmental samples is challenging due to their
62 low natural abundances (e.g upper crust abundance of Ta is about 0.9 ng kg⁻¹). This fact often
63 leads to difficulties regarding their quantification, resulting in expensive and time-consuming
64 sample preparation processes.^{7, 8, 11} Additionally, most methods are only suitable for the
65 analysis of a subset of the TCE group or the respective sample preparation processes are
66 confined to single elements.¹²⁻¹⁴ This situation necessitates new analytical methods for the
67 determination of multiple TCEs in environmental samples without the need for extensive
68 sample preparation.⁷

69 In environmental analysis, sediment or mineral samples are routinely analyzed. Sediments in
70 particular are considered a time record of environmental changes due to their potential to
71 accumulate contaminants over time. As sediments reflect the time-integrated status of the
72 aquatic environment, they are a powerful indicator to detect environmental changes in rivers,
73 estuaries or coastal areas over space and time.¹⁵⁻¹⁷ Therefore, the analysis of elemental mass
74 fractions in sediments is a common method for the assessment of long-term or emerging
75 contamination of aquatic systems. Nevertheless, acid digests of sediment samples also

1
2
3 76 represent an extremely complex sample matrix, often hindering the precise determination of
4
5 77 trace and ultra-trace analytes such as TCEs.¹⁷
6

7
8 78 Inductively coupled plasma mass spectrometry (ICP-MS) has proven to be the method of
9
10 79 choice for the determination of trace and ultra-trace elements in various environmental
11
12 80 matrices¹⁸⁻²⁰. ICP-MS allows for low detection limits (*LOD*) combined with high sample
13
14 81 throughput and outstanding multi-elemental capabilities. However, TCE analysis via ICP-MS
15
16 82 may be impeded by spectral interferences. These interferences are mainly isobaric, doubly
17
18 83 charged, or polyatomic ions with the same *m/z* as the analytes of interest. Notwithstanding, the
19
20 84 approach of inductively coupled plasma tandem mass spectrometry (ICP-MS/MS) allows to
21
22 85 overcome interferences by using different reaction or collision gases (e.g. O₂ or NH₃) and a
23
24 86 second quadrupole mass filter.

25
26 87 Various spectral interferences hampering the accurate determination of TCEs have been
27
28 88 reported (e.g. ¹⁴²Nd²⁺, ¹⁴²Ce²⁺, and ¹⁴¹Pr²⁺ for ⁷¹Ga⁺ or ¹¹⁵Sn⁺ for ¹¹⁵In⁺).^{2, 21} The quantification
29
30 89 of some TCEs is particularly challenging, if spectral interferences are created by other targeted
31
32 90 analytes, e.g. the determination of Ge (⁷²Ge⁺) suffers from doubly charged interferences of Nd
33
34 91 (¹⁴³Nd²⁺, ¹⁴⁴Nd²⁺) and Sm (¹⁴⁴Sm²⁺). Recent work proved that numerous interferences (e.g. of
35
36 92 the rare earth elements (REE)) can be resolved by using ICP-MS/MS and O₂ as reaction gas.²²⁻
37
38 93 ²⁴ Noteworthy, it has been demonstrated that the formation of REEO⁺ is significantly fostered
39
40 94 by using N₂O instead of O₂ as a reaction gas; thus, improving sensitivity and *LODs*.²⁵
41
42 95 Advantages of N₂O over O₂ in terms of serving as reaction gas are the preferred O transfer
43
44 96 reaction of N₂O to other ions. Due to the lower O-binding energy of N₂O reaction, enthalpies
45
46 97 for many analyses can be reduced. Herewith, higher reactions rates can be achieved when using
47
48 98 N₂O.^{24, 26} For instance, N₂O enables higher formation rates of the M+16 or M+32 product ions,
49
50 99 allowing to increase sensitivity and selectivity for elements like Ge, Eu, or Yb by enabling to
51
52 100 measure their respective oxides.^{25, 27-29}
53

54
55 101 The aim of this work was the development of a new ICP-MS/MS-based method for the
56
57 102 determination of TCEs with a special focus on Ga, Ge Nb, In, Te and Ta in sediment digests,
58
59 103 using N₂O as oxidizing reaction gas to selectively eliminate possible spectral interferences of
60
61 104 these analytes, to allow for a more selective and sensitive measurement.
62

63
64 105

106 **Experimental**

107 **Reagents and standards**

108 All preparatory laboratory work was performed in a class 10,000/1,000 clean room. Type I
109 reagent grade water ($>18.2 \text{ M}\Omega \text{ cm}$) was obtained from an ultra-pure water system consisting
110 of an Elix 3 module (Merck Millipore, Darmstadt, Germany), a Milli-Q element module
111 (Merck Millipore, Darmstadt, Germany), and a Q-POD element (Merck Millipore, Darmstadt,
112 Germany). Analytical grade HNO_3 (65% w/w, Fisher Scientific GmbH) and analytical grade
113 HCl (30% w/w, Carl Roth GmbH + Co. KG, Karlsruhe, Germany) were further purified either
114 by double sub-boiling in perfluoroalkoxy-polymer (PFA)-subboiling stills (DST-4000 & DST-
115 1000, Savillex, Minnesota, USA) operated under clean room conditions. HBF_4 (38% w/w,
116 Chem-Lab, Zedelgem, Belgium) was used in ultra-pure quality for sample digestion without
117 any further purification.

118 Single and multi-element solutions were prepared, using either single element standards (Carl
119 Roth GmbH, Karlsruhe, Germany or Sigma Aldrich, Missouri, USA) or custom-made multi-
120 element standards (all traceable to NIST standards) of different compositions (Inorganic
121 Ventures, Christiansburg, USA).

122 The reference marine sediment GBW 07313 (National Research Centre for Certified Reference
123 Materials, Beijing, China), the reference stream sediment GBW 07311 (National Research
124 Centre for Certified Reference Materials), and Basalt reference material BCR-2 (United States
125 Geological Survey Certificate of Analysis, Denver, USA) were used for method development
126 and validation.

127 **Instrumentation and measurement procedures**

128 Measurements were conducted using an Agilent 8900 ICP-MS/MS (Agilent Technologies,
129 Tokyo, Japan) coupled to an ESI SC-4 DX FAST discrete autosampler (Elemental Scientific,
130 Omaha, Nebraska, USA) equipped with an ultra-low penetration air (ULPA) filtration unit
131 (Elemental Scientific, Omaha, Nebraska, USA). O_2 , N_2O and the no Gas measurement modes
132 were employed during all experiments. However, the instrumental setup only allows measuring
133 with either O_2 or N_2O since both gases share the same recommended cell gas line (cell gas line
134 4 for corrosive gases). Therefore, if necessary, measurements were conducted two times to
135 gather information for both the O_2 and the N_2O mode. For each measurement, the instrument

136 was optimized using a tune solution containing Li, Co, Y, Ce, and Tl ($10 \mu\text{g L}^{-1}$). Optimal
 137 tuning conditions are enumerated in Table 1. An external calibration covering a concentration
 138 range from $0.1 \mu\text{g L}^{-1}$ to $100 \mu\text{g L}^{-1}$ (stabilized in 3% (w/w) HNO_3 and 1% (w/w) HCl) for all
 139 analytes was used for quantification of each element. Each solution for optimization and
 140 quantification was prepared from custom-made multi-element standards (Inorganic Ventures,
 141 Christiansburg, USA) on a daily basis. To monitor potential carry-over effects wash blanks of
 142 2% (w/w) HNO_3 were measured after each sample triplicate.

143 *Table 1 Standard ICP-MS/MS instrument and plasma parameters*

Parameter	Single MS	MS/MS	MS/MS
Used Cell Gases	None	O_2	N_2O
Nebulizer	Self-aspirating MicroFlow	PFA MicroFlow	Self-aspirating MicroFlow
Cell gas flow	None	20% ¹	10% ¹
Spray chamber Temperature	2°C	2°C	2°C
Interface cones	Nickel	Nickel	Nickel
RF Power	1550 W	1550 W	1550 W
RF Matching	1.80 V	1.80 V	1.80 V
Nebulizer flow rate	1.07 L min^{-1}	1.10 L min^{-1}	1.07 L min^{-1}
Makeup gas flow rate	0.12 L min^{-1}	0.11 L min^{-1}	0.12 L min^{-1}
Integration time	0.1 s	0.1 s	0.1 s
Extract lens 1	-11.8 V	-7.6 V	-11.5 V
Extract lens 2	-240.0 V	-215 V	-205.0 V
Omega bias	-150.0 V	-130 V	-130 V
Omega lens	7.6 V	5.8 V	6.6 V
Q1 entrance	-50.0 V	-50.0 V	-50.0 V
Q1 exit	1.0 V	3.0 V	3.0 V
Cell focus	-4.0 V	3.0 V	2.0 V
Cell entrance	-40 V	-40 V	-40 V

¹ relative to approx. 1.5 mL min^{-1} at 100%

Cell exit	-51 V	-51 V	-51 V
Deflect	15.2 V	7.8 V	8.2 V
Plate bias	-50 V	-50 V	-50 V
OctP bias	-8.0 V	-8.0 V	-0.5 V
Axial	0.0 V	1.0 V	1.0 V
Accelaration			
OctP RF	130 V	160 V	150 V
Energy	5.0 V	-5.0 V	-5.0 V
discrimination			

144 **Comparison between O₂ and N₂O as a reaction gas**

145 To compare the effectiveness of O₂ and N₂O as the oxidizing reaction gases for Ga, Ge, Nb,
 146 In, Te, REEs, and Ta product ion scans for each analyte were conducted. For this purpose, a
 147 multi-element solution (100 µg L⁻¹) was measured using the product ion scan option of the
 148 instrument. Here the first quadrupole (Q1) is adjusted to a specific *m/z*, allowing only ions of
 149 this *m/z* to enter the reaction cell. The second quadrupole is set to scan the entire spectrum from
 150 *m/z*=2 to *m/z*=275, thus measuring any potential product ions that may form in the reaction cell.
 151 For this kind of measurement, every analyte was measured on its recommended isotope to keep
 152 potential spectral interferences as low as possible. After each measurement, the ICP-MS/MS
 153 system was flushed with the respective reaction gas (O₂ or N₂O) by using a custom-made-
 154 flushing setup consisting of two 3 port valves allowing to flush the entire gas line bypassing
 155 the ICP-MS/MS. The gas lines were flushed for about half a minute using the respective gas.
 156 Afterwards, the cell was flushed for about 15 min setting the mass flow controller at 100% of
 157 the possible gas flow rate. For quantification of product ion formation rates, the relative
 158 formation rates were calculated by dividing the observed signal intensity of the product ion by
 159 the on-mass reference signal in the respective measuring mode.

160 **Effectiveness of N₂O to reduce possible interferences on Ga, Ge, Nb, In, Te, and Ta**

161 The effects of possible interferences (mainly doubly charged and oxide ions) on the
 162 determination of Ga, Ge, Nb, In, Te, and Ta, as well as the effectiveness of interference
 163 reduction by N₂O as the reaction gas, were analyzed by measuring single element standards
 164 (100 µg L⁻¹) or single-element solutions (*a*) spiked with their respective interfering elements
 165 (*i*) at ratios of *a/i*=1:10 and *a/i*=1:100. Within this context our work focused on these six

1
2
3 166 elements since earlier studies already emphasized that the measurement of REE as REEO⁺ will
4
5 167 significantly decrease potential interferences mainly caused by other REEO⁺.²²⁻²⁵ Each solution
6
7 168 was measured both in the no gas single quadrupole mode and in the MS/MS mode with N₂O
8
9 169 as a reaction gas. Relative signal intensities were used to quantify the influence of different
10
11 170 interferences and the effectiveness of interference reduction. The corresponding relative signal
12
13 171 intensities were calculated based on the signal of the unspiked single element solution in the
14
15 172 respective measuring mode (no gas or N₂O) as reference.

16 173 **Digestion procedure**

17
18
19 174 The digestion of each sediment reference material was accomplished via microwave-assisted
20
21 175 acid digestion using either a MARS Xpress or a MARS 6 (CEM Corp., Kamp Lintfort,
22
23 176 Germany) respectively following the digestion protocol developed by Zimmermann *et al.*
24
25 177 (2020).¹⁷ Briefly 50 mg of sediment were digested using a mixture of 5 mL HNO₃, 2 mL HCl
26
27 178 and 1 mL HBF₄ at 180°C for 300 min.

28 179 **Validation of optimized method using certified (sediment) reference materials**

29
30 180 Validation of the optimized method was carried out by means of the reference materials
31
32 181 GBW 07313, GBW 07311, and BCR-2. All analytes were measured using the single MS mode
33
34 182 with no additional cell gas, and using the MS/MS with N₂O in a single acquisition.

35 183 **Data processing and calculations**

36
37
38
39 184 Multi-element data was processed using MassHunter version 4.4 (Agilent Technologies,
40
41 185 Tokyo, Japan) in combination with a custom-written Excel[®] spreadsheet. Using this
42
43 186 spreadsheet, the respective limit of detection (*LOD*) ($3 \times SD$) and limit of quantification (*LOQ*)
44
45 187 ($3 * LOD$) of the method, were calculated based on the digestion blanks ($n=6$), as described by
46
47 188 MacDougall *et al.*.³⁰ Furthermore, expanded uncertainties with a coverage factor of 2 (U , $k=2$)
48
49 189 for each element present in the different reference materials were calculated using a simplified
50
51 190 *Kragten* approach following Reese *et al.* (2019).^{31, 32} For this purpose, the measurement
52
53 191 precision of the samples, as well as the reproducibility of multiple digests were taken into
54
55 192 account.

56 193 The significant number of digits of mass fractions are given according to GUM and
57
58 194 EURACHEM guidelines, whereby the uncertainty determines the significant number of digits
59
60 195 to be presented with the value.^{33, 34}

196 Results and Discussion

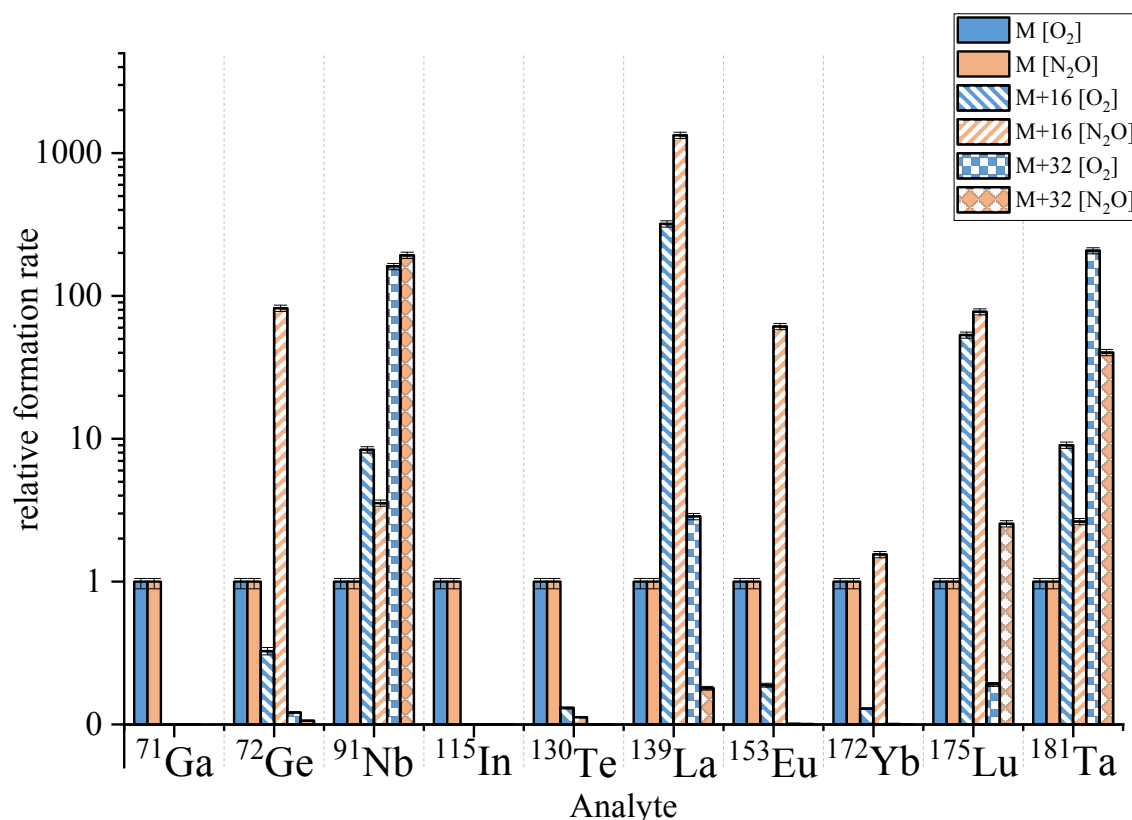
197 Product ion scans of selected TCEs using O₂ and N₂O as reaction gases

198 Figure 1 gives an overview of selected TCEs (Ga, Ge, Nb, In, Te, La, Eu, Yb, Lu, Ta) and their
199 relative oxide formation rates. Here Ga, Ge, Nb, Te and Ta represent TCEs with no information
200 on possible product ions using N₂O as reaction gas, while La, Eu, Yb and Lu were selected to
201 represent the REEs. Within this context La and Lu represent members of the light REE (LREE)
202 and heavy REE (HREE), respectively. Eu and Yb were included since both of them are known
203 to have low oxide formation rates when using O₂ as reaction gas.²⁹ Additional data for other
204 REEs can be found in ESI Table A.1. In Figure 1 color-coded columns display the M, M+16
205 as well as M+32 formation rates for the O₂ and N₂O measuring mode. Hence, it is possible to
206 directly compare the respective sensitivity for each ion. Scanning of possible product ions
207 revealed the preferable formation of oxides with a mass shift of M+16 or M+32 for most of the
208 tested analytes except for Ga, In and Te for which no significant oxide formation was observed.
209 Despite the insignificant oxide formation of Ga, In, and Te, Figure 1 illustrates absolute signal
210 intensities (cf. ESI Tabel A.1) showing that the usage of N₂O led to significantly higher signal
211 intensities for the M⁺ ion for each of the three elements. This indicates that a more sensitive
212 measurement of Ga, In and Te could be possible when using N₂O instead of O₂.

213 The other analytes showed oxide formation rates ranging from 0.1 (YbO⁺) for O₂ as reaction
214 gas to 1330 (LaO⁺) for N₂O as reaction gas. It becomes evident that Ge, La, Eu, Yb, and Lu
215 beared the highest relative oxide formation rates at M+16 ranging from 1.5 (Yb) to 1330 (La)
216 when N₂O was used as a reaction gas. However, the same elements only reached relative
217 formation rates of 0.1 (Yb) to 320 (La) once O₂ was used. This indicates that N₂O induces a
218 better O transfer for these five elements. This tendency was confirmed for all other REEs (ESI
219 tables A.1) except for Pr, Nd, Tb, Ho and Er. The improved oxide formation rate of N₂O was
220 particularly evident for the formation of EuO⁺ and GeO⁺. With respect to both elements, the
221 usage of O₂ as oxidation gas resulted in relative signals of 0.3 (EuO⁺) and 0.5 (GeO⁺) while
222 formation rates of 61 and 82 were achieved by using N₂O.

223 Nb and Ta preferred to form M+32 ions for both O₂ and N₂O as reaction gases. Figure 1 shows
224 relative formation rates of NbO₂⁺ for both O₂ (161) and N₂O (193), indicating that detection of
225 Nb clearly benefits from utilization of both gases. Similarly Ta preferred to form dioxides at
226 $m/z = 181+32$ with relative formation rates of around 207 (O₂) and 40 (N₂O) indicating that

227 other products (mostly N_2O cluster) are formed as well.²⁸ However, further measurements
 228 elucidated that the measurement of Ta as TaO^+ at $m/z = 197$ enables a more stable measurement
 229 despite lower sensitivity. Regarding all the above-mentioned elements, it is possible to exploit
 230 the mass shift mode to reduce or eliminate possible matrix-related spectral interferences.



231

232

233 *Figure 1 Comparison of the relative oxide formation rates for Ga, Ge, Nb, In, Te, La, Eu, Yb, Lu, and Ta and their main*
 234 *product ions in O₂ (blue) and N₂O (orange) measuring mode. All relative oxide formation rates refer to the absolute signal*
 235 *intensities in CPS of the respective element measured in the given gas mode.*

236 **Elimination of the most abundant interferences on Ga, Ge, Nb, In, Te and Ta using N₂O as a** 237 **reaction gas**

238 Detection of TCEs often suffers from spectral interferences making a precise measurement at
 239 sub-mg kg⁻¹ levels very challenging. Therefore eliminating these interferences in order to
 240 improve the sensitivity and selectivity of the measuring method is inevitable. Table 2 gives a
 241 short overview of the respective TCEs (Ga, Ge, Nb, In, Te and Ta) and their most abundant or
 242 often occurring interferences when analyzing environmental matrices. Since previous studies
 243 already have shown, that the measurement of REE as REEO⁺ can reduce the negative effects
 244 of interfering elements (mainly other REEO⁺) and the fact that N₂O leads to better oxide

245

246

247

248

249

250

245 formation for the REEs the following section focuses on the improved determination of the
 246 TCEs Ga, Ge, Nb, In, Te and Ta.

247
 248

Table 2 Overview of measured isotopes of Ga, Ge, Nb, In, Te and Ta and their most abundant spectral interferences

Analyte	Interference
^{71}Ga	$^{142}\text{Nd}^{2+}$, $^{142}\text{Ce}^{2+}$, $^{141}\text{Pr}^{2+}$, $(^{55}\text{Mn}^{16}\text{O})^+$, $(^{40}\text{Ar}^{31}\text{P})^+$
^{72}Ge	$^{143}\text{Nd}^{2+}$, $^{144}\text{Nd}^{2+}$, $^{144}\text{Sm}^{2+}$, $(^{56}\text{Fe}^{16}\text{O})^+$, $(^{40}\text{Ar}^{32}\text{S})^+$, $(^{40}\text{Ca}^{16}\text{O}_2)^+$
^{93}Nb	$^{186}\text{W}^{2+}$, $(^{40}\text{Ar}^{53}\text{Cr})^+$
^{115}In	$^{115}\text{Sn}^+$, $(^{40}\text{Ar}^{75}\text{As})^+$
^{130}Te	$^{130}\text{Ba}^+$, $^{130}\text{Xe}^+$, $(^{114}\text{Cd}^{16}\text{O})^+$
^{181}Ta	$(^{165}\text{Ho}^{16}\text{O})^+$

249
 250 Figure 2 compares the relative signal intensities of single element solutions of Ga, Ge, Nb, In,
 251 Te and Ta in the no gas and N_2O measurement modes. Besides, the respective analyte solutions
 252 (a) were spiked with interfering elements (i) at two different ratios ($a/i=1:10$ and $a/i=1:100$).
 253 This setup enabled the evaluation of the possible influence of interferences as summarized in
 254 Table 2. It provides a good comparison of possible sensitivity or selectivity enhancements
 255 when using N_2O as a reaction gas.

256 Figure 2a shows that the presence of Nd and Ce in a ratio of 1:100 has a large effect on the
 257 signal intensity of ^{71}Ga in the no gas mode. The intensity increased by almost 27% (Nd) and
 258 16% (Ce), which is caused by the formation of doubly charged Nd^{2+} and Ce^{2+} in the plasma. In
 259 the N_2O MS/MS mode, these interferences can be overcome since Nd^{2+} and Ce^{2+} are no longer
 260 able to pass the second quadrupole, as they will react to MO^{2+} or MO^+ in MS/MS mode, thus
 261 ensuring an interference-free measurement on $m/z=71$ for Ga. Whereas the potential
 262 interference caused by Pr^{2+} proved to be insignificant in the N_2O mode for the tested elemental
 263 ratios.

264 A similar pattern was observed for ^{72}Ge (Figure 2b). In this case, Nd (1:100 ratio) may lead to
 265 an increasing signal of ^{72}Ge when measuring in the no gas mode. In contrast, Sm^{2+} seems to
 266 have no significant influence on the determination of ^{72}Ge due to the lower isotopic abundance
 267 of ^{144}Sm . Measurements of ^{72}Ge and the accordingly spiked Ge samples investigated in the
 268 N_2O mode revealed the possibility to eliminate Nd^{2+} interferences by detection of $^{72}\text{Ge}^+$ as

269 $^{72}\text{Ge}^{16}\text{O}^+$ (mass shift from $m/z=72$ to $m/z=88$). While, Nd^{2+} will be discriminated as $^{144}\text{Nd}^{16}\text{O}_2^+$
270 and $^{144}\text{Nd}^{16}\text{O}^+$ or as $^{143}\text{Nd}^{16}\text{O}_2^+$ and $^{143}\text{Nd}^{16}\text{O}^+$, respectively.

271 Figure 2c shows, that W may hamper an accurate analysis of Nb either in the no gas or N_2O
272 mode. A W induced signal suppression can be observed for both measuring modes leading to
273 the hypothesis that the signal suppression may take place inside the ion source itself. Even
274 though the interference effect of W on Nb could not be improved by using N_2O as reaction gas,
275 it is safe to say that the analysis of Nb still benefits from the MS/MS mode as W/Nb in
276 environmental matrices may be < 5 leading to a non-significant change in the measured
277 intensities. Furthermore, a measurement of Nb as NbO_2^+ will also help to overcome other
278 possible polyatomic interferences like $(\text{ArMn})^+$, $(\text{ArFe})^+$, or $(\text{ArCr})^+$.

279 As shown in Figure 2e, the determination of ^{130}Te is massively impaired by the isobaric
280 interference of ^{130}Ba in the no gas mode. At a spike ratio of 1:100, an increase of the signal by
281 factor 2 was observed. In the N_2O mode, Ba^+ reacts to BaO^+ , which allows an interference-free
282 measurement of ^{130}Te .

283 Figure 2d shows that both the no gas and the N_2O mode will lead to a ^{115}Sn interference-free
284 detection of ^{115}In up to a spike ratio of at least 1:10. In both modes, the signal intensity increased
285 slightly for a spike ratio of 1:100. This can be expected due to the low natural abundance of
286 ^{115}Sn (0.34%) and high natural abundance of ^{115}In (95.7%). The effect of Ho on the
287 measurement of ^{181}Ta showed an unusual behaviour. Here the lower spiked solution (1:10)
288 showed a significant intensity increase for Ta while the higher spiked solution showed a signal
289 reduction. This pattern is evident for both measuring modes (no gas and N_2O) again leading to
290 the conclusion that in that the effect may take place in the ion source.

291 The N_2O MS/MS mode shows the potential to significantly reduce the influence of isobaric
292 and polyatomic interferences for the elements Ga, Ge and Te. This also offers the possibility to
293 analyze more abundant isotopes. Thus, leading to improved sensitivities e.g. in the case of
294 ^{130}Te . For Nb, and Ta little to no improvement can be observed for the tested interferences (W,
295 Sn and Ho), but we are convinced, that the measurement in the N_2O mode will still lead to
296 improved results since other polyatomic interferences will be eliminated by the use of the mass
297 shift mode.

298

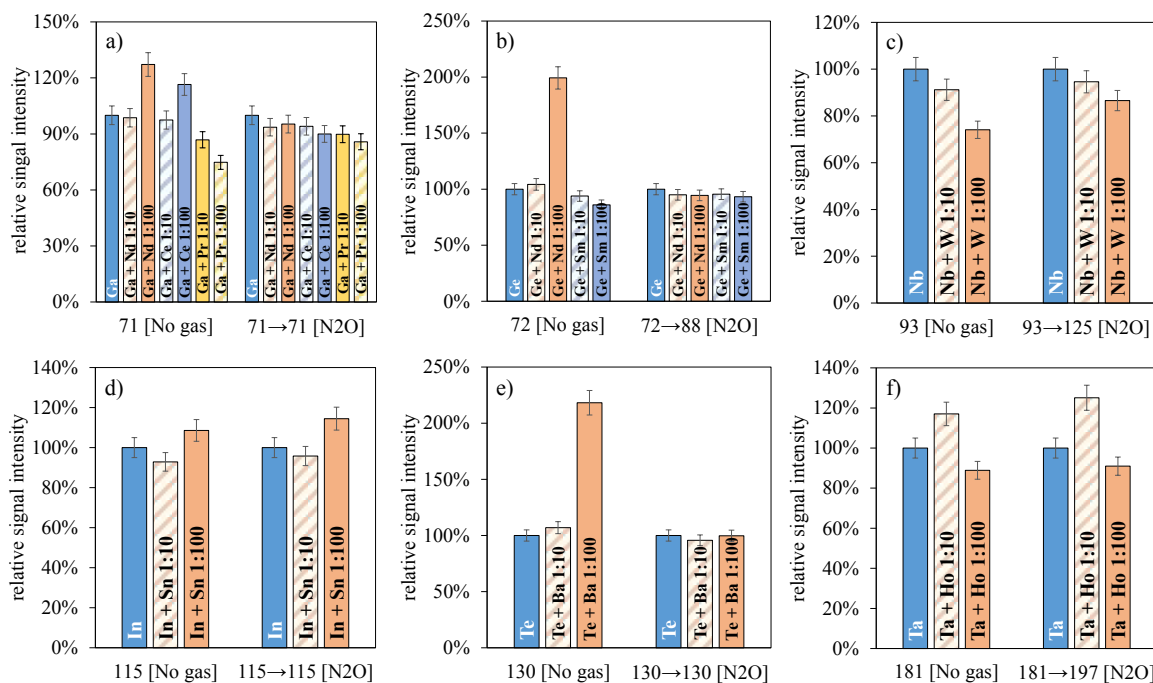


Figure 2 Comparison of the relative signal changes in the no gas mode and N₂O mode of a) Ga, b) Ge, c) Nb, d) In, e) Te, and f) Ta in the presence of their most frequent interferences, spiked in different ratios (1:10 and 1:100). All relative signals in percent refer to the absolute signal in CPS of the corresponding measurement of the single element solution in the respective measurement mode.

Limits of quantification and recoveries of TCEs in digests of certified reference materials

Acid digests of the reference materials BCR-2, GBW 07311, and GBW 07313 were measured using the developed method to determine the accuracy and recoveries for the individual analytes. The provided *LODs* and *LOQs* are based on six method blank values. Table 3 shows a comparison of the calculated *LODs* for each measured TCE in single MS no gas mode and in MS/MS mode using either O₂ or N₂O.

The measurement of TCEs in the MS/MS modes (O₂ and N₂O) led to an improved or at least similar *LOD* compared to the no gas mode. Only La, Sm, Tb, Dy, Er and Ta show lower *LODs* in the no gas mode. Even though these six elements do not show improved *LODs* in one of the MS/MS modes it is highly recommended to use the mass shift mode since it ensures the removal of earlier discussed spectral interferences. Additionally, it is evident that for these elements the N₂O mode often provides *LODs* within the same range as the *LODs* of the no gas mode (e.g. La: $LOD_{no\ gas} = 0.006\ \mu\text{g L}^{-1}$, $LOD_{N_2O} = 0.006\ \mu\text{g L}^{-1}$ or Tb: $LOD_{no\ gas} = 0.0004\ \mu\text{g L}^{-1}$, $LOD_{N_2O} = 0.0004\ \mu\text{g L}^{-1}$).

In general it is evident, that the N₂O mode with the exception of Sc, Ga, In and Te always features lower *LODs* compared to the O₂ mode. Nevertheless, the *LODs* for Sc, Ga and In in the N₂O mode (Sc: $0.010\ \mu\text{g L}^{-1}$, Ga: $0.04\ \mu\text{g L}^{-1}$ and In: $0.013\ \mu\text{g L}^{-1}$) lay within the same

range of their respective *LODs* in the O₂ mode (Sc: 0.008 µg L⁻¹, Ga: 0.023 µg L⁻¹ and In: 0.012 µg L⁻¹). Te shows a significantly higher *LOD* in the N₂O mode (0.13 µg L⁻¹) when compared to both other measuring modes which is caused by the ¹³⁰Xe interference on ¹³⁰Te. *LOD* may be improved by either using higher gas flows of N₂O or by with increasing energy discrimination voltage. Yet, all other analytes of interest exhibit better oxide formation rates or sensitivities for the parameters given in Table 1, hence the resulting inferior *LOD* of Te was a necessary compromise.

Overall, the best *LOD* improvements by using N₂O are achieved for Ge and Nb (Ge: 0.024 µg L⁻¹ compared to 0.051 µg L⁻¹ (no gas) and 0.045 µg L⁻¹ (O₂ mode); Nb: 0.023 µg L⁻¹ compared to 0.028 µg L⁻¹ (O₂ mode)).

Table 4 lists measured elemental mass fractions of selected TCEs and recoveries for the analysis of three reference materials (GBW 07311, BCR-2 and GBW 07313). Recoveries of the developed method ranged between 72% to 106% for GBW 07311, 87% to 107% for BCR-2 and 69% to 112% for GBW 07313. Under consideration of the calculated uncertainties of the measurement, as well as given uncertainties of the reference materials, the determination of all analytes can be assumed accurate as long as recoveries range between 70% and 120%.

For Nb, the reference material GBW 07313 shows a recovery of only 69%. However, the given reference value does not feature any information regarding the exact uncertainty.

Recoveries of Te for the reference material GBW 07311 were significantly higher (185%) than certified. This is in accordance with Zimmermann *et al.* (2020)¹⁷ who found a similar recovery rate, which the authors measured in single MS mode as ¹²⁵Te. Therefore, it can be assumed that the isobaric interference of ¹³⁰Ba on ¹³⁰Te does not explain the non-quantitative recovery. One explanation for the significantly higher recovery rate may be an carbon induced signal enhancement as described by Grindlay *et al.* (2013).³⁵ It is predicted that in presence of carbon some hard-to-ionize analytes like Sb, Te, Au, Se, As, Hg, I and P may experience a signal enhancement during ICP-MS measurements mainly induced by possible charge transfer reactions of C⁺ or CO⁺ ions.³⁵ The total carbon content of the reference material is about 0.24%, which may already lead to an enhanced Te signal. For further validation a multi-element in house standard² without additional carbon was measured and screened for Te (*n* = 12). For this

² This standard contains the Elements: Ag, Al, As, B, Ba, Be, Bi, Ca, Cd, Co, Cr, Cu, Fe, Ga, Hg, In, K, Li, Mg, Mn, Mo, Na, Ni, Pb, Rb, , Sb Se, Sn, Sr, Te, Ti, Tl, U, V, Zn, REE at either 25.00 µg L⁻¹, 250.0 µg L⁻¹ or 2500 µg L⁻¹

standard Te showed a recovery of 94% ($m_{\text{measurement}} = 24 \mu\text{g L}^{-1} \pm 6 \mu\text{g L}^{-1}$, $c_{\text{reference}} = 25.0 \mu\text{g L}^{-1} \pm 1.3 \mu\text{g L}^{-1}$) indicating an accurate measurement.

To summarize, our results prove that all analytes give accurate and reproducible results using the presented method. It should be noted, that the development of multi-element methods often result in compromises with regard to e.g. *LODs* or *LOQs* as it is rarely possible to find the perfect method parameter for all analytes simultaneously. Therefore, potentially slightly better *LODs* or *LOQs* may be achieved in single-element analysis.

Table 3 *LODs* and of all measured elements in no gas, O₂ and N₂O mode. The respective elements were measured either in single MS (only Q1) mode or MS/MS mode (Q1 and Q2)

Analyte	Q1	Q2	single MS	MS/MS O ₂	MS/MS N ₂ O
			<i>LOD</i> / $\mu\text{g L}^{-1}$	<i>LOD</i> / $\mu\text{g L}^{-1}$	<i>LOD</i> / $\mu\text{g L}^{-1}$
Sc	45	61	0.7	0.008	0.010
Ga	71	71	0.04	0.023	0.04
Ge	72	88	0.05	0.05	0.024
Y	89	105	0.02	0.019	0.017
Nb	93	125	0.012	0.0028	0.0023
In	115	115	0.016	0.012	0.013
Te	130	130	0.06	0.012	0.13
La	139	155	0.006	0.008	0.006
Ce	140	156	0.011	0.011	0.009
Pr	141	157	0.0010	0.0015	0.0013
Nd	146	162	0.004	0.004	0.0028
Sm	147	163	0.0008	0.0022	0.0011
Eu	153	169	0.0003	0.0006	0.00023
Gd	157	173	0.0015	0.0016	0.0014
Tb	159	175	0.0004	0.001	0.0004
Dy	163	179	0.0024	0.004	0.003
Ho	165	181	0.0006	0.0012	0.0006
Er	166	182	0.0021	0.0027	0.0023
Tm	169	185	0.0004	0.0012	0.00029
Yb	172	188	0.0026	0.004	0.0016
Lu	175	191	0.0006	0.0010	0.0004

365 Table 4 Measured and certified mass fractions of the analyzed reference materials GBW 07311 ($n=7$), GBW 07313 ($n=4$) and BCR-2 ($n=10$). Errors correspond to expanded uncertainties (U ,
 366 $k=2$). All italicized values are either information values provided on the certificates or from references 36, 35, and 38.³⁶⁻³⁸

Analyte	GBW 07311 ($n=7$)			BCR-2 ($n=10$)			GBW 07313 ($n=4$)		
	certified range / mg kg ⁻¹	measured / mg kg ⁻¹	recovery	certified range / mg kg ⁻¹	measured / mg kg ⁻¹	recovery	certified range / mg kg ⁻¹	measured / mg kg ⁻¹	recovery
Sc	7.4 ± 0.4	5 ± 3	72%	33 ± 2	29 ± 11	87%	25.6 ± 2.9	28.8 ± 2.4	112%
Ga	18.5 ± 0.9	20 ± 5	106%	23 ± 2	23 ± 4	100%	23.7 ± 1.7	22.2 ± 2.2	94%
Ge	1.81 ± 0.21	1.9 ± 0.7	103%	<i>1.46³⁶ ± 0.26³⁶</i>	1.48 ± 0.33	102%		2.12 ± 0.23	
Y	43 ± 5	36 ± 9	82%	37 ± 2	35 ± 5	95%	104 ± 5	107 ± 13	103%
Nb	25.0 ± 3.0	25 ± 6	101%	<i>12.41³⁶ ± 0.02³⁶</i>	11.4 ± 1.9	91%	<i>15.1</i>	10.4 ± 1.1	69%
In	1.9 ± 0.3	1.8 ± 0.5	97%	<i>0.09127³⁷ ± 0.00094³⁷</i>	0.087 ± 0.016	95%		0.139 ± 0.017	
Te	0.4 ± 0.1	0.74 ± 0.19	185%	<i>0.004³⁶</i>	< LOD	-		3.04 ± 0.28	
La	30 ± 2	30 ± 8	100%	25 ± 1	27 ± 4	107%	67.8 ± 2.9	68 ± 8	101%
Ce	58 ± 4	61 ± 13	105%	53 ± 2	55 ± 8	104%	92 ± 8	92 ± 11	100%
Pr	7.4 ± 0.5	7.3 ± 1.7	98%	6.8 ± 0.3	7.2 ± 1.4	105%	20.1 ± 1.9	20.6 ± 2.5	103%
Nd	27 ± 2	26 ± 7	98%	28 ± 2	30 ± 6	106%	92 ± 4	86 ± 8	94%
Sm	6.2 ± 0.3	6.0 ± 1.8	97%	6.7 ± 0.3	6.5 ± 1.2	98%	21.5 ± 1.3	18.5 ± 2.0	86%
Eu	0.6 ± 0.06	0.57 ± 0.16	94%	2.0 ± 0.1	1.9 ± 0.3	97%	5.3 ± 0.3	4.6 ± 0.6	86%
Gd	5.9 ± 0.4	5.7 ± 1.7	97%	6.8 ± 0.3	7.0 ± 1.2	102%	22.0 ± 1.2	20.3 ± 1.9	92%
Tb	1.13 ± 0.09	0.95 ± 0.28	84%	1.07 ± 0.04	1.02 ± 0.16	95%	3.4 ± 0.3	3.0 ± 0.4	87%
Dy	7.2 ± 0.6	6.1 ± 1.9	84%		6.4 ± 1.0	-	19.9 ± 1.8	18.1 ± 2.4	91%
Ho	1.4 ± 0.2	1.2 ± 0.37	85%	1.33 ± 0.06	1.26 ± 0.16	95%	4.3 ± 0.2	3.5 ± 0.5	81%

Analyte	GBW 07311 (<i>n</i> =7)			BCR-2 (<i>n</i> =10)			GBW 07313 (<i>n</i> =4)		
	certified range / mg kg ⁻¹	measured / mg kg ⁻¹	recovery	certified range / mg kg ⁻¹	measured / mg kg ⁻¹	recovery	certified range / mg kg ⁻¹	measured / mg kg ⁻¹	recovery
Er	4.6 ± 0.5	3.6 ± 1.1	78%		3.6 ± 0.5	-	11.0 ± 0.7	9.7 ± 1.2	88%
Tm	0.74 ± 0.09	0.57 ± 0.17	77%	0.54	0.50 ± 0.07	93%	1.54 ± 0.14	1.36 ± 0.20	89%
Yb	5.1 ± 0.6	3.9 ± 1.2	77%	3.5 ± 0.2	3.2 ± 0.5	92%	9.8 ± 1.1	8.8 ± 1.2	89%
Lu	0.78 ± 0.06	0.60 ± 0.21	77%	0.51 ± 0.02	0.51 ± 0.09	99%	1.46 ± 0.19	1.32 ± 0.16	91%
Ta	5.7 ± 0.5	5.0 ± 0.9	88%	0.79 ^a ± 0.02 ^a	0.70 ± 0.21	89%	1.11 ³⁸ ± 0.13 ³⁸	0.81 ± 0.07	73%

367

Published on 19 May 2021. Downloaded on 5/20/2021 7:05:44 AM.

Journal of Analytical Atomic Spectrometry Accepted Manuscript

368 **Conclusion**

369 The developed approach of measuring TCEs in sediment digests by ICP-MS/MS using N₂O as
370 a reaction gas allows the quasi-simultaneous and accurate analysis of Ga, Ge, Nb, In, Te, Ta as
371 well as REEs. For at least one of the measured reference material, recoveries ranging from 80%
372 to 112% could be achieved for all analytes. Additionally, *LODs* and *LOQs* of Ge, Y, Nb, Ce,
373 Nd, Eu, Gd, Ho, Tm, Yb, and Lu were significantly improved by means of N₂O as a reaction
374 gas, since possible interferences (e.g. Nd²⁺ or Sm²⁺) can be effectively removed.

375 Consequently, the new method enables the determination of elemental mass fractions of TCEs
376 in sediment samples, which can help to gain better insights into the behavior of these elements
377 in the marine environment or to determine their origin, fate and distribution within complex
378 land-river-sea systems. Validated analytical workflows are of great importance to understand
379 the future role of TCEs as potential emerging inorganic contaminants. Furthermore, the N₂O
380 gas mode may be easily implemented in already existing ICP-MS/MS multi-element methods
381 to analyze not only TCEs/REEs, but other elements are also deemed to benefit from oxide
382 formation such as Ti, Mo, or W. Therefore, we propose to replace O₂ by N₂O as standard
383 oxidizing agent in ICP-MS/MS measurements, due to significantly higher oxide formation
384 rates observed for many elements.

385 In a future applications in the frame of environmental studies, our method will be used to
386 investigate the input of TCEs into the environment, with special emphasis on In and Ga inputs,
387 from offshore wind farms in the German Bight, which play a key role in the ongoing energy
388 transition in Germany to achieve the sustainable development goals of the United Nations.
389 Therefore, the general background concentrations of the individual TCEs in the German Bight
390 will be investigated as well as the extent to which offshore wind farms represent sources for
391 TCEs affecting their surrounding environment.

392

1
2
3 393 **Conflict of interest**
4
5

6 394 The authors have no competing interests to declare.
7
8

9 395 **Acknowledgment**
10

11 396 The authors would like to thank Madita Kruse for her support in the laboratory.
12
13

14 397
15
16
17
18
19
20
21
22
23
24
25
26
27
28
29
30
31
32
33
34
35
36
37
38
39
40
41
42
43
44
45
46
47
48
49
50
51
52
53
54
55
56
57
58
59
60

398

399 **Bibliographic references**

- 400 1. M. Filella and J. C. Rodriguez-Murillo, *Chemosphere*, 2017, **182**, 605-616.
- 401 2. M. Filella and I. Rodushkin, *Spectrosc. Acta Pt. B-Atom. Spectr.*, 2018, **141**, 80-84.
- 402 3. P. Nuss and G. A. Blengini, *Sci Total Environ*, 2018, **613-614**, 569-578.
- 403 4. A. Reese, N. Voigt, T. Zimmermann, J. Irrgeher and D. Profrock, *Chemosphere*,
- 404 2020, **257**, 127182.
- 405 5. L. T. Peiró, G. V. Méndez and R. U. Ayres, *Environmental science & technology*,
- 406 2013, **47**, 2939-2947.
- 407 6. A. Cobelo-Garcia, M. Filella, P. Croot, C. Frazzoli, G. Du Laing, N. Ospina-Alvarez,
- 408 S. Rauch, P. Salaun, J. Schafer and S. Zimmermann, *Environ Sci Pollut Res Int*,
- 409 2015, **22**, 15188-15194.
- 410 7. M. Romero-Freire, J. Santos-Echeandia, P. Neira and A. Cobelo-Garcia, *Frontiers in*
- 411 *Marine Science*, 2019, **6**.
- 412 8. M. G. Barth, W. F. McDonough and R. L. Rudnick, *Chemical Geology*, 2000, **165**,
- 413 197-213.
- 414 9. L. Grandell, A. Lehtila, M. Kivinen, T. Koljonen, S. Kihlman and L. S. Lauri,
- 415 *Renewable Energy*, 2016, **95**, 53-62.
- 416 10. M. Jabłońska-Czapla and K. Grygoyć, *Polish Journal of Environmental Studies*,
- 417 2021, **30**, 1477-1486.
- 418 11. R. Rudnick and S. Gao, *The crust*, 2003, **3**, 1-64.
- 419 12. Y. Lu, A. Makishima and E. Nakamura, *Chemical Geology*, 2007, **236**, 13-26.
- 420 13. K. Nagaishi and T. Ishikawa, *Geochemical Journal*, 2009, **43**, 133-141.
- 421 14. M. Krachler, C. Mohl, H. Emons and W. Shotyk, *Journal of Analytical Atomic*
- 422 *Spectrometry*, 2002, **17**, 844-851.
- 423 15. F. Ackermann, H. Bergmann and U. Schleichert, *Environmental Technology Letters*,
- 424 2008, **4**, 317-328.
- 425 16. U. Förstner, in *Chemical methods for assessing bio-available metals in sludges and*
- 426 *soils*, eds. R. Leschber, R. D. Davis and P. L'Hermite, Elsevier Science Pub. Co.,
- 427 Inc., New York, NY, United States, 1985, pp. 1-30.
- 428 17. T. Zimmermann, M. von der Au, A. Reese, O. Klein, L. Hildebrandt and D. Profrock,
- 429 *Anal Methods*, 2020, **12**, 3778-3787.
- 430 18. L. Balcaen, E. Bolea-Fernandez, M. Resano and F. Vanhaecke, *Analytica chimica*
- 431 *acta*, 2015, **894**, 7-19.
- 432 19. E. Bolea-Fernandez, L. Balcaen, M. Resano and F. Vanhaecke, *Journal of Analytical*
- 433 *Atomic Spectrometry*, 2017, **32**, 1660-1679.
- 434 20. D. Profrock and A. Prange, *Applied spectroscopy*, 2012, **66**, 843-868.
- 435 21. I. Wysocka, *Talanta*, 2021, **221**, 121636.
- 436 22. K. Nakano, *Direct measurement of trace rare earth elements in high purity REE*
- 437 *oxides*, Agilent Technologies Inc., 2015.
- 438 23. N. Sugiyama and G. Woods, *Direct measurement of trace rare earth elements*
- 439 *(REEs) in high-purity REE oxide using the Agilent 8800 Triple Quadrupole ICP-MS*
- 440 *with MS*, 2012.
- 441 24. Agilent Technologies Inc., *Agilent 8800 Triple Quadrupole ICP-MS: Understanding*
- 442 *oxygen reaction mode in ICP-MS/MS*, 2012.
- 443 25. N. Sugiyama, *Direct Analysis of Ultratrace Rare Earth Elements in Environmental*
- 444 *Waters by ICP-QQQ*, 2020.
- 445 26. V. H. Dibeler, *Journal of Chemical Physics*, 1967, **47**, 2191-&.
- 446 27. G. K. Koyanagi, D. Caraiman, V. Blagojevic and D. K. Bohme, *The Journal of*
- 447 *Physical Chemistry A*, 2002, **106**, 4581-4590.
- 448 28. V. V. Lavrov, V. Blagojevic, G. K. Koyanagi, G. Orlova and D. K. Bohme, *The Journal*
- 449 *of Physical Chemistry A*, 2004, **108**, 5610-5624.

- 1
2
3 450 29. G. K. Koyanagi and D. K. Bohme, *The Journal of Physical Chemistry A*, 2001, **105**,
4 451 8964-8968.
5 452 30. D. MacDougall, W. B. Crummett and et al., *Analytical Chemistry*, 1980, **52**, 2242-
6 453 2249.
7 454 31. A. Reese, T. Zimmermann, D. Pröfrock and J. Irrgeher, *Science of the total*
8 455 *environment*, 2019, **668**, 512-523.
9 456 32. J. Kragten, *Analyst*, 1994, **119**, 2161-2165.
10 457 33. S. L. Ellison and A. Williams, *Quantifying uncertainty in analytical measurement*, 3
11 458 edn., 2012.
12 459 34. S. L. R. Ellison, B. Magnusson and U. Örnemark, *Eurachem Guide: Template for*
13 460 *Eurachem Guides - A Guide for Guide Editors*, 1 edn., 2015.
14 461 35. G. Grindlay, J. Mora, M. de Loos-Vollebregt and F. Vanhaecke, *Spectrochimica Acta*
15 462 *Part B: Atomic Spectroscopy*, 2013, **86**, 42-49.
16 463 36. K. P. Jochum, U. Weis, B. Schwager, B. Stoll, S. A. Wilson, G. H. Haug, M. O.
17 464 Andreae and J. Enzweiler, *Geostandards and Geoanalytical Research*, 2016, **40**,
18 465 333-350.
19 466 37. M. Kirchenbaur, A. Heuser, A. Bragagni and F. Wombacher, *Geostandards and*
20 467 *Geoanalytical Research*, 2018, **42**, 361-377.
21 468 38. M. Balla, Z. Molnar and A. Koros, *Journal of Radioanalytical and Nuclear Chemistry*,
22 469 2004, **259**, 395-400.
23
24 470
25
26 471
27
28
29
30
31
32
33
34
35
36
37
38
39
40
41
42
43
44
45
46
47
48
49
50
51
52
53
54
55
56
57
58
59
60